Evidence of large nuclear deformation of $^{32}S^*$ formed in the $^{20}Ne + ^{12}C$ reaction

Aparajita Dey, S. Bhattacharya, C. Bhattacharya, K. Banerjee, T. K. Rana, S. Kundu, S. Mukhopadhyay, D. Gupta, and R. Saha

Variable Energy Cyclotron Centre, 1/AF Bidhan Nagar, Kolkata 700064, India

(Received 3 January 2006; revised manuscript received 9 May 2006; published 19 October 2006)

Deformations of hot composite $^{32}S^*$ formed in the reaction ^{20}Ne(∼7–10 MeV/nucleon) + ^{12}C have been estimated from the respective inclusive α-particle evaporation spectra. The estimated deformations for $^{32}S^*$ have been found to be much larger than the "normal" deformations of hot, rotating composites at similar excitations. This further confirms the formation of a highly deformed long-lived configuration of $^{20}Ne + ^{12}C$ at high excitations (∼70–100 MeV)—which was recently indicated from analysis of complex fragment emission data for the same system. Exclusive α-particle evaporation spectra from the decay of hot composite $^{32}S^*$ also show similar behavior.

DOI: 10.1103/PhysRevC.74.044605 PACS number(s): 24.60.Dr, 25.70.Pq, 25.70.Jj, 27.30.+t

I. INTRODUCTION

The phenomena of clustering and large deformations in light $N = Z$ nuclei has recently evoked a lot of interest and a few attempts have been made to study the characteristics of such light, highly deformed systems [1–4]. Formation of a long-lived, highly deformed dinuclear configuration has been observed in low-energy, light heavy-ion-induced reactions involving α-like nuclei [5]. These highly deformed systems are generally believed to be formed through the nuclear orbiting mechanism. Orbiting can be described in terms of the formation of a long-lived dinuclear complex that acts as a "doorway" state to fusion with a strong memory of the entrance channel—though the dynamics is not yet completely understood. It is particularly of interest to know how the deformed dinuclear shape (and vis-á-vis the orbiting process) evolves with increasing excitation energy. Various theoretical calculations also predict the formation of such highly deformed shapes of light mass ($A < 100$) $N = Z$ nuclei at higher excitation energy and angular momentum [6,7]. Recently, it has been reported that, for ^{20}Ne (∼ 7–10 MeV/nucleon) + ^{12}C reactions, yields of carbon and boron fragments are significantly enhanced [8], which may be indicative of the survival of orbiting at these high excitation energies (∼70–100 MeV); as orbiting is associated with the formation of a highly deformed dinuclear configuration, it will be interesting to investigate the quantitative deformation of the hot composites produced in the same reactions independently through other available experimental tools.

Light-charged-particle (LCP; $Z \leqslant 2$) spectroscopy is now-a-days routinely used to study the statistical properties of hot rotating nuclei [9]. In the case of compound nuclei at moderate energies and angular momenta, such as those produced with light-ion projectiles, the experimental spectra are well reproduced in terms of statistical models that employ the standard optical model transmission coefficients. However, in the case of heavy-ion-induced fusion reactions, that is, at high excitation energies and angular momenta, the energy spectra of evaporated light charged particles are no longer consistent with the standard statistical model predictions [9–15]. The discrepancy is believed to be due to the deformation of the composite system at high excitation energy and angular momentum, and proper modification of the emission barrier and/or the level density is needed to incorporate the effect of deformation [11–16]. Apart from that, entrance channel dynamics may also affect the evaporative decay if the composite forms a long-lived, highly deformed configuration (as observed in the reactions involving light α-like nuclei) with lifetime comparable to the evaporation time scale. Thus the LCPs in general (and αs in particular, as they are emitted predominantly at the initial stages of the decay cascade) can provide important clues about the nuclear deformation at high excitation energy and spin. This prompted us to explore the quantitative deformation of the $^{20}Ne + ^{12}C$ dinuclear system in the incident energy range ∼7–10 MeV/nucleon from the respective α-evaporation spectra.

In the present work, we have populated the hot composite nucleus $^{32}S^*$ in the excitation energy range ∼73.0–94.0 MeV through the $^{20}Ne + ^{12}C$ reaction at different bombarding energies. Inclusive energy and angular distributions of all the light charged particles have been measured. In-plane coincidence of light charged particles with both evaporation residues (ERs) and intermediate mass fragments (IMFs) has been measured at one incident energy (158 MeV) for comparison of inclusive and exclusive LCP emission spectra. Inclusive energy and angular distributions of the LCPs emitted from the hot composite formed in ^{20}Ne (158 MeV) + ^{27}Al reactions have also been measured. The deformations of the hot composites formed in these reactions have been estimated from the study of the respective α-evaporation spectra. It is found that the deformations of hot composites formed in the $^{20}Ne + ^{12}C$ reaction are much larger than the "normal" deformations, which hot, rotating compound nuclei (i.e., $^{31}P^*$ and $^{47}V^*$, formed in $^{19}F + ^{12}C$ [9] and $^{20}Ne + ^{27}Al$ reactions, respectively) may undergo at similar excitations. This further corroborates the conjecture of the formation of a highly deformed, long-lived configuration of the $^{20}Ne + ^{12}C$ system at high excitations, which was earlier indicated from the enhancement of fragment yield from the same system at these energies.

The paper has been arranged as follows. The experimental procedures are described in Sec. II. The analysis of the data and the results are discussed in Sec. III. Finally, a summary and concluding remarks are given in Sec. IV.

II. EXPERIMENTAL DETAILS

The experiments were performed with accelerated ^{20}Ne ion beams of energies of 145, 158, 170, 180, and 200 MeV, respectively, from the Variable Energy Cyclotron at Kolkata. The targets used were $\sim$550 μg/cm^2 self-supporting ^{12}C and $\sim$500 μg/cm^2 ^{27}Al foil. The IMFs and evaporation residues have been detected using two solid state $\Delta E - E$ [$\sim$10 μm Si(SB) ΔE, $\sim$300 μm Si(SB) E] telescopes (THI) mounted on one arm of the 91.5-cm scattering chamber. The light charged particles have been detected using two solid state thick detector telescopes [$\sim$40, 100 μm Si(SB) ΔE, $\sim$5 mm Si(Li) E] (TLI) mounted on the other arm of the scattering chamber. Typical solid angles subtended by the telescopes were 0.33, 0.19, 0.74, and 0.53 msr, respectively. The telescopes were calibrated using elastically scattered ^{20}Ne ions from Au, Al, and C targets and a ^{228}Th-α source. Absolute energy calibrations of the E and ΔE detectors for each telescope were done separately using standard kinematics and energy-loss calculations. The measured energies have been corrected for the energy losses at the target by incorporating a single average thickness correction for each fragment energy. The low-energy cutoffs thus obtained were typically $\sim$3.0 MeV for protons and $\sim$10.2 MeV for α particles in the TLI telescopes. In the THI telescopes, the cutoffs were $\sim$12.3 MeV for boron and $\sim$19.5 MeV for oxygen. Well-separated bands corresponding to elements having atomic numbers up to $Z = 13$ have been identified.

Inclusive energy distributions for light charged particles ($Z = 1, 2$) have been measured in the angular range 10°–50°, in steps of 2.5°, for ^{20}Ne + ^{12}C at all the bombarding energies and for ^{20}Ne + ^{27}Al at 158 MeV. We have also measured the in-plane coincidence of light charged particles with IMFs and ERs for ^{20}Ne + ^{12}C at 158 MeV for the comparison of inclusive and exclusive spectra.

III. RESULTS AND DISCUSSION

A. Energy distribution

Typical inclusive energy spectra of α-particles have been shown in Fig. 1 (left) for a 200-MeV bombarding energy. The energy spectrum at $\theta_{\rm lab} = 10°$ (filled circles) is compared with that at 50° (open circles). It is clearly seen from the figure that the slopes of the two spectra match well.

The shapes of the inclusive α-particle spectra have been compared with the respective exclusive spectra (coincident with ER, $Z = 10$–13) at $\theta_{\rm lab} = 15°$, 20°, 35°, and 40° in Fig. 2 (left panel). It is found that the shapes of the inclusive and exclusive α-particle spectra match well for all the angles.

In heavy-ion collisions with bombarding energies well above the Coulomb barrier, a significant fraction of the LCPs (particularly protons) is known to be emitted at forward angles in the early stage of the reaction [17]. The forward-angle LCP energy distributions have strong enhancement in the high-energy part when compared with those of evaporation spectra expected in compound nuclear reactions. This extra contribution in the forward direction is generally a signature of precompound emission, and it becomes insignificant at

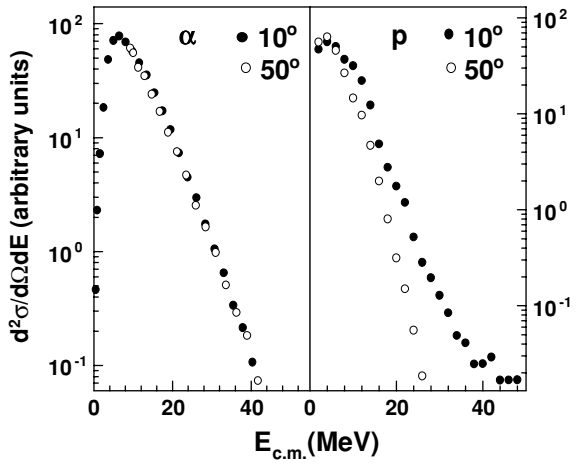

FIG. 1. Comparison of energy spectra of α particles (left) and protons (right) at two angles for the reaction ^{20}Ne ($E_{\rm lab}$ = 200 MeV) + ^{12}C.

$\theta_{\rm lab} > 30°$ in most of the cases. The proton energy spectra at 10° and 50° are displayed in Fig. 1 (right) for the reaction ^{20}Ne (200 MeV) + ^{12}C. It is evident that there is a significant contribution from pre-equilibrium processes at forward angles, so far as proton emission is concerned. In contrast, it is clear

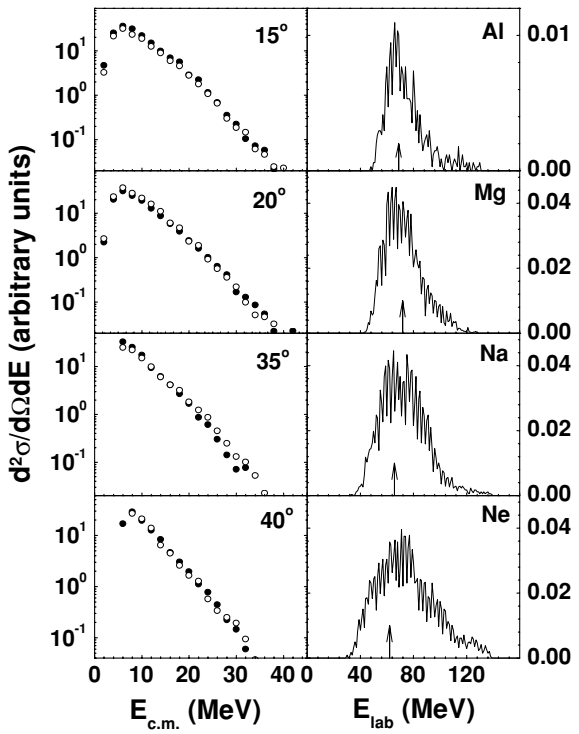

FIG. 2. (Left) Comparison between inclusive (filled circles) and exclusive (open circles, measured in coincidence with all ERs emitted at $\theta_{\rm lab} = 10°$) spectra for α particles at $E_{\rm lab} = 158$ MeV at different angles. Cross sections were normalized at one point for comparison. (Right) Evaporation residues spectra at $\theta_{\rm lab} = 10°$ measured in coincidence with LCPs (see text). The arrow indicates the energy corresponding to the residue velocity $\simeq v_{\rm CN} \cos\theta_{\rm lab}$ for the respective ER.

from Figs. 1 (left) and 2 that pre-equilibrium emission does not have any significant effect on the α-particle emission spectra. The in-plane coincidence spectra of ERs (measured at $\theta_{\rm lab} = 10^\circ$) with LCPs (measured at $\theta_{\rm lab} = 40^\circ$) have been shown in Fig. 2 (right panel). It is seen that all the ER spectra peak at energies corresponding to those of completely fused residues moving with velocity $\simeq v_{\rm CN}\cos\theta_{\rm lab}$ (indicated by the arrow); $V_{\rm CN}$ is the compound nucleus velocity. It is thus clearly evident that the α-particles are emitted predominantly from the evaporative decay of the hot composite.

B. Invariant cross section

The velocity contour maps of the Galilean-invariant differential cross sections, $(d^2\sigma/d\Omega dE)p^{-1}c^{-1}$, as a function of the velocity of the emitted α-particles provide an overall picture of the reaction pattern. Figure 3 shows these velocity diagrams of invariant cross sections in the $(v_\parallel, v_\perp)$ plane for α-particles emitted at different incident energies. The arrows indicate the compound nucleus velocity, $v_{\rm CN}$. The circles correspond to the most probable average velocities. It has been observed that, for all incident energies, the average velocities fall on a circle around the compound nucleus velocity. This implies that the average velocities (as well as kinetic energies) of the αs are independent of the center-of-mass (c.m.) emission angles. This is an indication of complete energy relaxation and emission of charged particles from a fully equilibrated source moving with velocity $v_{\rm CN}$.

C. Statistical model analysis

The experimental energy spectra of α-particles for a few representative laboratory angles (i.e., 10° and 30° for 145 MeV and 10°, 30°, and 50° for other bombarding energies) are displayed in Fig. 4. The open circles represent the inclusive experimental data. At each emission angle the energy spectra exhibit approximately exponential slopes. The shapes and high-energy slopes of the spectra are essentially independent of the c.m. emission angle. This is a signature of a statistical de-excitation process arising from a thermalized source and the exponential slope may be used to extract the source temperature.

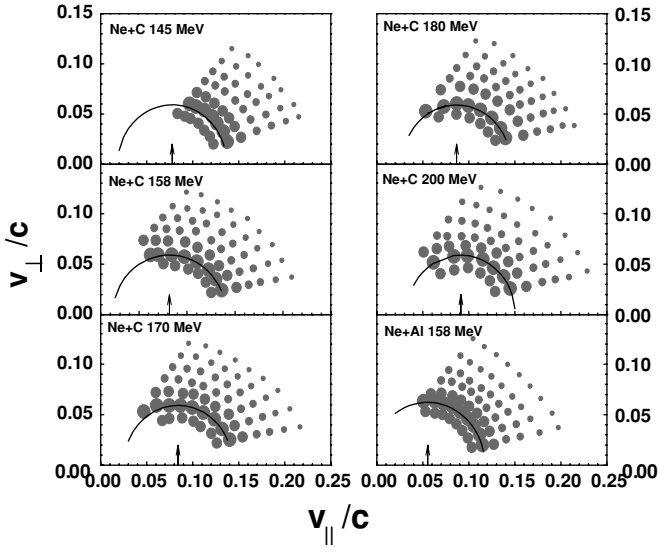

FIG. 3. The invariant cross section of α particles plotted in the $(v_\parallel, v_\perp)$ plane at different energies. The size of the point is in proportion to the invariant cross section. The arrow corresponds to the compound nucleus velocity ($v_{\rm CN}$) for each energy. Solid curves are the most probable average velocities.

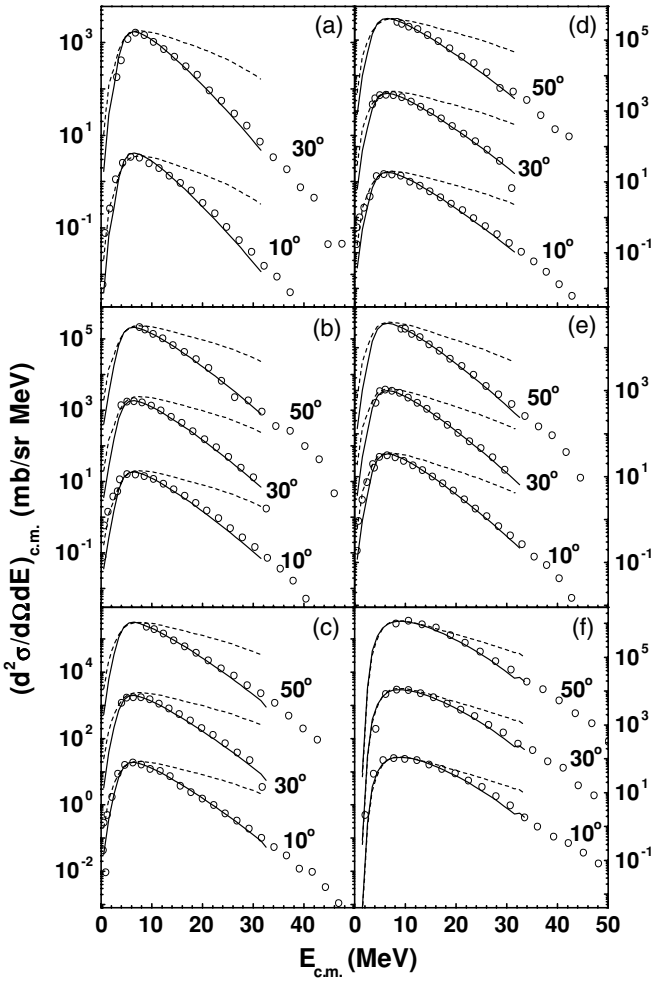

FIG. 4. Inclusive energy spectra for α particles at incident energies of (a) 145 MeV, (b) 158 MeV, (c) 170 MeV, (d) 180 MeV, and (e) 200 MeV for the system ^{20}Ne + ^{12}C and (f) 158 MeV for the ^{20}Ne + ^{27}Al system at laboratory angles of 10° ($\times 10^{-2}$), 30° ($\times 10^{0}$), and 50° ($\times 10^{2}$), respectively. Open circles represent the experimental data. Dashed (solid) curves are the predictions of the statistical model code CASCADE without (with) deformation (see text).

The analysis of the data (^{20}Ne + ^{12}C) has been performed using the standard statistical model code CASCADE [18]. The dashed lines in Fig. 4 represent the predictions of the statistical model code CASCADE. The optical-model parameters used for calculating the transmission coefficients were taken from Perey and Perey [19] for protons and from Huizenga and Igo [20] for α-particles. The critical angular momentum for fusion, $j_{\rm cr}$, was calculated using the Bass model [21] for each bombarding energy. The radius parameter r_0 was taken

to be 1.29 fm, following Pühlhofer *et al.* [18]. The angular-momentum-dependent deformation parameters (δ_1 and δ_2 as described later) were set equal to zero [13]. From Fig. 4, it is clear that the theoretical calculations fail to predict the overall shape of the experimental spectra over the whole energy range.

In the statistical model calculations, the lower energy part of the LCP spectrum is controlled by the transmission coefficients. However, the high-energy part of the spectrum depends crucially on the available phase space obtained from the level densities at high spin. In hot rotating nuclei formed through heavy-ion reactions, the nuclear level density at high angular momentum is taken to be spin dependent. For the calculation of transmission coefficients, we have used the optical-model parameters, as mentioned earlier. A deformed configuration of the compound nucleus has been assumed in the calculation. This is realized by varying the radius parameter r_0 as well as the deformation parameters δ_1, δ_2 of the spin-dependent moment of inertia (as explained later in the text). The optimum value of r_0 is found to be $\sim$1.35 fm. The increased radius parameter lowers the emission barrier and hence enhances the low-energy yield by increasing the transmission coefficients. The high-energy part of the spectrum is controlled by the level density $\rho(E^*, j)$. For a given angular momentum j and excitation energy E^*, the level density is defined as [13,18]

$$\rho(E^*, j) = \frac{(2j+1)}{12} a^{1/2} \left(\frac{\hbar^2}{2\mathcal{I}_{\text{eff}}}\right)^{3/2} \frac{1}{(E^* + T - \Delta - E_j)^2} \times \exp\left[2[a(E^* - \Delta - E_j)]^{1/2}\right], \quad (1)$$

where a (taken as $A/8$, with A being the mass number of the hot rotating nucleus) is the level density parameter, T is the thermodynamic temperature, Δ is the pairing correction, and E_j is the rotational energy, which can be written in terms of effective moment of inertia $\mathcal{I}_{\text{eff}}$ as

$$E_j = \frac{\hbar^2}{2\mathcal{I}_{\text{eff}}} j(j+1). \quad (2)$$

In hot rotating nuclei, formed through heavy-ion reactions, the effective moment of inertia is taken to be spin dependent and is written as

$$\mathcal{I}_{\text{eff}} = \mathcal{I}_0 \times (1 + \delta_1 j^2 + \delta_2 j^4), \quad (3)$$

where the rigid-body moment of inertia, $\mathcal{I}_0$, is given by

$$\mathcal{I}_0 = \tfrac{2}{5} A^{5/3} r_0^2. \quad (4)$$

Nonzero values of the parameters δ_1, δ_2 introduce the spin dependence in the effective moment of inertia. The relation (2) defines a region in the energy-angular momentum plane (E-j plane) of allowed levels, which is bounded by the yrast line, the locus of the lowest energy states corresponding to each angular momenta. It has been observed in previous experiments [9,12,13,22] that the yrast line has to be modified by varying the radius and deformation parameters r_0, δ_1, and δ_2 to explain the experimental data.

In the present work, the radius parameter r_0 was varied from 1.29 to 1.35 fm to take care of the low-energy side of the experimental spectra. In addition, the variation of spin-dependent level density parameters was also needed for explaining the high-energy side of the spectra. This procedure is illustrated in Fig. 5 for the ^{20}Ne (200 MeV) + ^{12}C reaction at an angle $\theta_{\text{lab}} = 10^\circ$, where calculations with three different sets of parameters are displayed to highlight the roles played by different parameters in explaining the data. It is clearly seen (see inset of Fig. 5) that the change of r_0 from 1.29 to 1.35 fm causes a shift of the peak of the distribution to the low-energy side and thus helps to fit the lower energy part of the data in a better way. For different bombarding energies, different sets of δ_1, δ_2 values were needed. The parameter δ_1 plays the main role in explaining the high-energy part of the data; it is also found to be quite sensitive to variation of the excitation energy of the system. However, a nonzero value of the parameter δ_2 is required to fit the high-energy-tail ($\gtrsim$ 20 MeV) part of the data in particular, and it is found to be rather insensitive, to the variation of excitation energy, at least within the range of the present measurements. Optimum values of the parameters may, however, vary from system to system. The optimized values of radius and deformation parameters are given in Table I. It is clearly seen that the experimental spectra are well explained with these values (solid lines in Fig. 4). The exclusive α-particle spectra at $\theta_{\text{lab}} = 15^\circ$, 20°, 35°, and 40° are given in Fig. 6. These α-particle spectra were measured in coincidence with ERs ($10 \leqslant Z \leqslant 13$). It is seen that the exclusive spectra are also well explained with the same set of parameters ($r_0 = 1.35$ fm, $\delta_1 = 4.5 \times 10^{-3}$, and $\delta_2 = 2.0 \times 10^{-8}$) as those obtained for the inclusive data at the same energy.

From the preceding analyses, it is clear that a large amount of spin-dependent deformation is needed to explain the emitted α spectra from the ^{20}Ne + ^{12}C reaction. It will be interesting

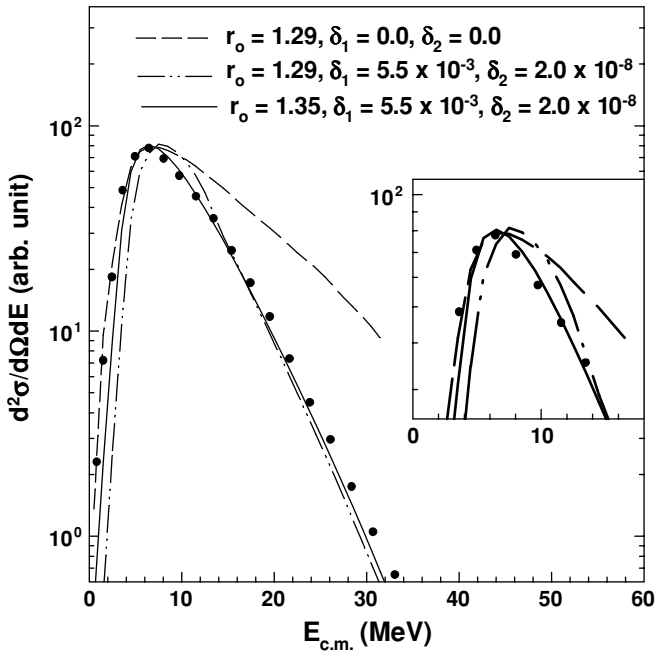

FIG. 5. Experimental α-particle energy spectrum (filled circles) at 10° for the ^{20}Ne (200 MeV) + ^{12}C reaction compared with different CASCADE predictions. Variation near the peak of the distribution is shown in the inset.

TABLE I. The optimized value of deformation parameters at each incident energy.

E_{lab} (MeV)	E^* (MeV)	j_{cr} ($\hbar$)	r_0 (fm)	δ_1	δ_2	r_{eff} (fm)
145[a]	73	24	1.35	3.7×10^{-3}	2.0×10^{-8}	1.95
158[a]	78	24	1.35	4.5×10^{-3}	2.0×10^{-8}	2.06
170[a]	82	24	1.35	5.0×10^{-3}	2.0×10^{-8}	2.12
180[a]	86	25	1.35	5.2×10^{-3}	2.0×10^{-8}	2.20
200[a]	94	25	1.35	5.5×10^{-3}	2.0×10^{-8}	2.24
158[b]	108	38	1.30	4.5×10^{-4}	2.0×10^{-8}	1.51
96[c]	60	21	1.29	2.8×10^{-3}	2.5×10^{-7}	1.65

[a]→ ^{20}Ne + ^{12}C system.
[b]→ ^{20}Ne + ^{27}Al system.
[c]→ ^{19}F + ^{12}C system [9].

to compare these deformations with those obtained for other non-α-like light nuclei at similar excitation energy and spin. Two representative systems [^{47}V* and ^{31}P*, formed in ^{20}Ne (158 MeV) + ^{27}Al and ^{19}F (96 MeV) + ^{12}C [9], respectively] were considered for the purpose of comparison. The inclusive α-energy spectra for the decay of ^{47}V* are shown in Fig. 4 along with the CASCADE prediction. The optimized values of the deformation parameters for both ^{47}V* and ^{31}P* are given in Table I. The deformation parameters for both systems are found to be very different from those obtained for the decay of ^{32}S*.

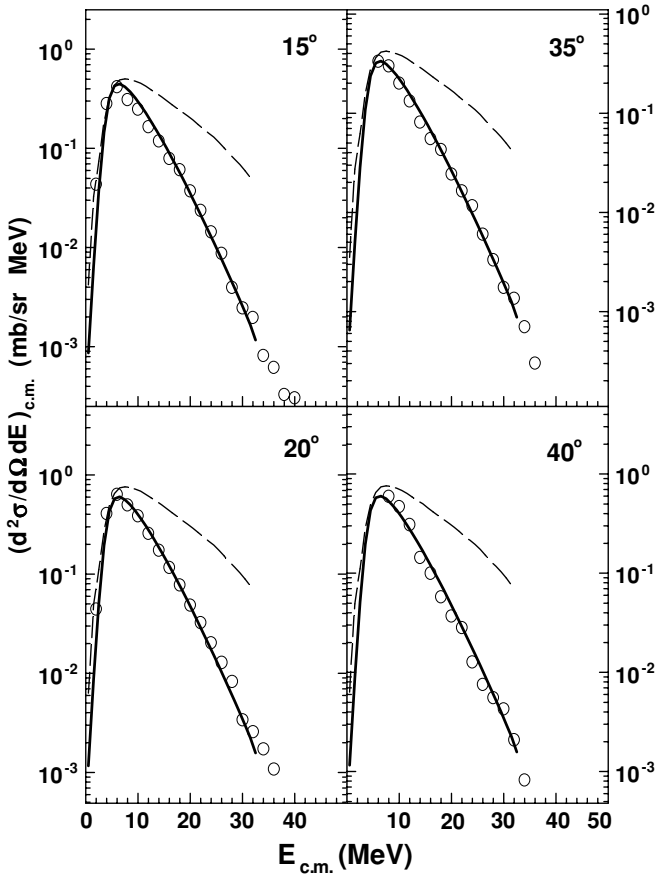

FIG. 6. Exclusive α-particle spectra at different θ_{lab} measured in coincidence with ERs emitted at $\theta_{lab} = 10^\circ$ in the ^{20}Ne (158 MeV) + ^{12}C reaction. Open circles are the experimental points; dashed (solid) curves are CASCADE predictions without (with) deformation.

A more quantitative comparison of effective deformations of the hot composites studied here can be made by examining the values of effective radius parameters (r_{eff}) obtained from the analysis of the data. The effective radius parameters (for nonzero values of δ_1 and δ_2 given in Table I) were estimated by averaging over the angular-momentum distribution (by assuming a sharp cutoff triangular distribution, up to the critical angular momentum, j_{cr}) in the following way:

$$r_{eff}^2 = r_0^2 \frac{\Sigma_0^{j_{cr}}(1 + \delta_1 j^2 + \delta_2 j^4)(2j+1)}{\Sigma_0^{j_{cr}}(2j+1)}. \quad (5)$$

The estimated values of the effective radius parameters are given in Table I. It is seen that r_{eff} (and deformation) increases with increasing excitation energy. It is further observed that values of r_{eff} for the ^{20}Ne + ^{12}C system at all energies are significantly larger than those for the two representative non-α-like systems (^{19}F + ^{12}C and ^{20}Ne + ^{27}Al), even though in one case (^{20}Ne + ^{27}Al) the angular momentum involved is much larger. This clearly indicates that the deformations of the hot composites formed in ^{20}Ne + ^{12}C reactions are larger than those for other light non-α-like systems at similar excitation energies.

IV. SUMMARY AND CONCLUSION

It has been observed that α-particles are emitted predominantly from equilibrated compound nuclear sources in all the reactions studied here. However, the experimentally measured spectra deviate significantly from the standard statistical model predictions. A significant amount of deformation is needed to explain the measured spectra satisfactorily. A deformed configuration of the compound nucleus is considered through the modification of the radius parameter r_0 from 1.29 to 1.35 fm and by varying the spin-dependent level density parameters δ_1 and δ_2. It is evident that deformations needed to explain the α spectra from the ^{20}Ne + ^{12}C system are significantly larger than those needed for the ^{20}Ne + ^{27}Al and ^{19}F + ^{12}C systems. Effective radius parameters extracted for the ^{20}Ne + ^{12}C system are also significantly larger than those extracted for non-α-like ^{19}F + ^{12}C and ^{20}Ne + ^{27}Al systems—indicating larger overall deformations in the ^{20}Ne + ^{12}C system. This may be another signature of the formation of a long-lived orbiting-like dinuclear system at higher excitation energies (∼70–100 MeV) in the ^{20}Ne + ^{12}C reaction, which was indicated earlier [8] from fragment emission studies.

ACKNOWLEDGMENTS

The authors thank the cyclotron operating crew for smooth running of the machine and H. P. Sil for the fabrication of thin silicon detectors for the experiment. One of the authors (A.D.) acknowledges with thanks the financial support provided by the Council of Scientific and Industrial Research, Government of India.

[1] H. Horiuchi, Y. Kanada-En'yo, and M. Kimura, Nucl. Phys. **A722**, 80c (2003).
[2] H. Horiuchi, Nucl. Phys. **A731**, 329 (2004).
[3] W. von Oertzen *et al*., in *Book of Abstracts, International Nuclear Physics Conference, Göteborg, Sweden, June 27–July 02, 2004,* TC61.
[4] S. Thummerer *et al*., J. Phys. G **27**, 1405 (2001).
[5] S. J. Sanders, A. Szanto de Toledo, and C. Beck, Phys. Rep. **311**, 487 (1999) and references therein.
[6] S. Aberg and L. O. Joensson, Z. Phys. A **349**, 205 (1994).
[7] J. Zhang, A. C. Merchant, and W. D. M. Rae, Phys. Rev. C **49**, 562 (1994).
[8] C. Bhattacharya *et al*., Phys. Rev. C **72**, 021601(R) (2005).
[9] D. Bandyopadhyay, C. Bhattacharya, K. Krishan, S. Bhattacharya, S. K. Basu, A. Chatterjee, S. Kailas, A. Srivastava, and K. Mahata, Eur. Phys. J. A **14**, 53 (2002) and references therein.
[10] R. K. Choudhurry *et al*., Phys. Lett. **B143**, 74 (1984).
[11] G. La Rana, D. J. Möses, W. E. Parker, M. Kaplan, D. Logan, R. Lacey, J. M. Alexander, and R. J. Welberry, Phys. Rev. C **35**, 373 (1987).
[12] G. Viesti, B. Fornal, D. Fabris, K. Hagel, J. B. Natowitz, G. Nebbia, G. Prete, and F. Trotti, Phys. Rev. C **38**, 2640 (1988).
[13] J. R. Huizenga, A. N. Behkami, I. M. Govil, W. U. Schröder, and J. Tõke, Phys. Rev. C **40**, 668 (1989).
[14] B. Fornal *et al*., Phys. Rev. C **41**, 127 (1990).
[15] M. Rousseau *et al*., Phys. Rev. C **66**, 034612 (2002).
[16] W. E. Parker *et al*., Phys. Rev. C **44**, 774 (1991).
[17] T. C. Awes *et al*., Phys. Rev. C **24**, 89 (1981).
[18] F. Pühlhofer, Nucl. Phys. **A280**, 267 (1977).
[19] C. M. Perey and F. G. Perey, At. Data Nucl. Data Tables **17**, 1 (1976).
[20] J. R. Huizenga and G. Igo, Nucl. Phys. **29**, 462 (1962).
[21] R. Bass, *Nuclear Reactions with Heavy Ions* (Springer-Verlag, Berlin, 1980), p. 256.
[22] C. Bhattacharya *et al*., Phys. Rev. C **65**, 014611 (2001).